

**CHARACTERIZATION OF 2-DIMENSIONAL  
ELECTRICAL RESISTIVITY TOMOGRAPHY,  
GEOTECHNICAL AND HYDRAULIC  
CONDUCTIVITY ANALYSIS IN THE GRANITIC  
RESIDUAL SOIL**

**OLADUNJOYE PETER OLABODE**

**UNIVERSITI SAINS MALAYSIA**

**2021**

**CHARACTERIZATION OF 2-DIMENSIONAL  
ELECTRICAL RESISTIVITY TOMOGRAPHY,  
GEOTECHNICAL AND HYDRAULIC  
CONDUCTIVITY ANALYSIS IN THE GRANITIC  
RESIDUAL SOIL**

by

**OLADUNJOYE PETER OLABODE**

**Thesis submitted in fulfilment of the requirement  
for the degree of  
Doctor of Philosophy**

**December 2021**

## ACKNOWLEDGEMENT

I thank GOD ALMIGHTY for the opportunity given to me to pursue a doctoral degree. I dedicated this work to my mother Late Mrs. Mathilda Olayotu Olabode whose effort through my upbringing inspire me to reach this educational height. I thank my father Late Benjamin Olabode. I would like to express my sincere gratitude to my wife Mrs Ifedayo Omolola Olabode, whose care and love keep me strong throughout the research work and my children Odunayo Deborah Olabode, Mary Oreofe Elizabeth Olabode, Iyanuoluwa Ruth Opemipo Olabode and Oluwasegun Daniel Olabode. I would also thank my siblings Mrs Wumi Adeola Akinmoju, Mrs Mofeoluwa Roseline Ojo, Mrs Olayemi Margreth and Miss Ileola Olabode.

My profound gratitude goes to my supervisor Associate Professor Hwee Lim San for his support and guidance throughout the research work. I also thank my co-supervisor Dr. Muhd Harris Ramli for his immense contribution and guidance. I appreciate the assistance of Dr. Nordiana Muztaza. I acknowledge my colleague Abubakar for his timely assistance during my fieldwork. I appreciate my other colleagues Dr. Damilola Samson, Sani Muhammed and Dakok Kyermang Kyense.

I also appreciate the cooperation of the field support of the technical staff of Geophysics Section, School of Physics Messers Shahil Ahmad Khosaini, Yakuub Bin Othman and Azmi bin Abdullah and the technical staff of Geotechnical laboratory of the School of Civil Engineering Messers Zabidi and other staffs.

Special thanks to Prof. Martins Olorunfemi, Prof. I. B. Osazuwa, Late Associate Prof. J. O. Fatoba and Prof. (Mrs) C. I. Akintayo.

I would like to thank the Federal University Oye-Ekiti and The Federal Government of Nigeria for granting me the study leave and their financial support.

# TABLE OF CONTENTS

<b>ACKNOWLEDGEMENT.....</b>	<b>ii</b>
<b>TABLE OF CONTENTS.....</b>	<b>iii</b>
<b>LIST OF TABLES.....</b>	<b>vii</b>
<b>LIST OF FIGURES.....</b>	<b>viii</b>
<b>LIST OF ABBREVIATIONS.....</b>	<b>xii</b>
<b>LIST OF SYMBOLS.....</b>	<b>xiii</b>
<b>ABSTRAK.....</b>	<b>xvii</b>
<b>ABSTRACT.....</b>	<b>xix</b>
<b>CHAPTER 1 INTRODUCTION.....</b>	<b>1</b>
1.1 Overview of Background.....	1
1.2 Problem Statement.....	5
1.3 Aim and Objectives.....	7
1.4 Scope of the Study.....	7
1.5 Significant of the Study.....	9
1.6 Thesis Structure.....	10
<b>CHAPTER 2 LITERATURE REVIEW.....</b>	<b>11</b>
2.1 Introduction.....	11
2.2 Previous Studies.....	12
2.3 Review of the Electrical Resistivity Method.....	16
2.3.1 Basic Theory of Electrical Resistivity.....	16
2.3.2 Data Acquisition .....	21
2.3.2(a) Traditional 1-D Resistivity Method.....	21

2.3.2(b)	Two and Three-Dimensional Resistivity Methods.....	23
2.3.2(b)(ii)	Multi-electrode Resistivity Systems: Electrical Resistivity Tomography.....	23
2.4	Review of Geotechnical Techniques.....	28
2.4.1	Phase Relationships: Soil Water Content .....	28
2.4.2	Determination of Hydraulic Conductivity.....	30
2.4.2(a)	Laboratory Determination of hydraulic conductivity.....	30
2.4.2(b)	Empirically Derived of Hydraulic Conductivity.....	34
2.4.3	Determination of Shear Strength.....	36
2.5	Slope Stability, Slope Instability and Slope Failure.....	36
2.5.1	Slope Instability and Geology of Weathered Basement rocks.....	37
2.5.2	Impact of Climate on Slope Instability.....	40
2.5.3	Weathering and Weathering Profile in a Typical Basement Environment.....	40
2.5.3(a)	Weathering profile .....	41
2.5.3(a)(i)	Hydrogeology of a Weathering Profile .....	44
2.5.3(b)	Hydraulic Conductivity and Soil Resistivity.....	46
2.5.4	Water Infiltration and Recharge System.....	50
2.6	Percentage Deviation Error.....	51
2.7	Chapter summary.....	51
<b>CHAPTER 3 MATERIALS AND METHODS.....</b>		<b>52</b>
3.1	Study Area.....	52
3.1.1	Site Selection.....	52
3.1.2	Site Description.....	54
3.1.2	Geology and Soil Characterisation.....	56

3.1.4	Precipitation, Temperature and Relative Humidity Data.....	57
3.2	Data Acquisition.....	57
3.2.1	ERT Data Acquisition.....	59
3.2.2	Geotechnical Laboratory Tests.....	63
3.2.2(a)	Moisture Content.....	63
3.2.2(b)	Density.....	64
3.2.2(c)	Laboratory Determination of Hydraulic Conductivity.....	64
3.2.2(d)	Determination of Shear Strength.....	65
3.2.2(d)(i)	Direct Shear Test Procedure.....	66
3.2.3	Hydrogeological data Collection for estimation of Hydraulic Conductivity.....	67
3.2.3(a)	Particle size distribution.....	68
3.3	Percentage Deviation Error.....	71
3.4	Chapter summary.....	71
<b>CHAPTER 4 RESULTS AND DISCUSSION.....</b>		<b>73</b>
4.1	Analysis of the Climatic Data of the Study Area.....	73
4.2	Analysis of Geotechnical-assisted 2-D Electrical Resistivity Tomography (ERT) Monitoring of Slope Instability in Residual Soil of Weathered Granitic Basement.....	75
4.2.1	ERT Models Interpretation.....	75
4.2.2	Geotechnical Interpretation.....	83
4.3	Analysis of 2-D Electrical Resistivity Tomography (ERT) and Engineering Properties for Slope Instability Monitoring in Residual Soil of Weathered Granitic Basement.....	87
4.3.1	Electrical Resistivity Tomography Model.....	87
4.3.2	Geotechnical Laboratory Test.....	93
4.4	Hydrogeological Assessment of Soil Piping Development on Hill Slope Soil for Slope Instability Monitoring.....	101

4.4.1	ERT model result.....	102
4.4.2	Geotechnical Parameters Analysis.....	105
4.4.2(a)	Soil Piping.....	105
4.4.2(b)	Moisture Content.....	109
4.4.2(c)	Particle Size Distribution and Empirical Derived Hydraulic Conductivities.....	109
4.4.2(d)	Laboratory Determined Hydraulic Conductivity.....	118
4.4.2(e)	Hydraulic Conductivity Versus Soil Resistivity.....	120
4.5	Chapter summary.....	123
<b>CHAPTER 5 CONCLUSION AND RECOMMENDATIONS.....</b>		<b>125</b>
5.1	Conclusion.....	125
5.2	Recommendation for Future Work.....	129
<b>REFERENCES.....</b>		<b>130</b>
<b>LIST OF PUBLICATIONS</b>		

## LIST OF TABLES

	<b>Page</b>
Table 3.1	Selected Sieve Sizes Based on Grain Size.....69
Table 4.1	Climatic Data for the Months of Jan. 2019 to Feb. 2020.....74
Table 4.2	Characteristics of The Six (6) ERT Profiles Acquired Using 42 Steel Electrodes with Wenner-Schlumberger Array.....77
Table 4.3	Classification of ERT Inverted Models on The Scale of Resistivity Values into Zones.....77
Table 4.4	Summarized Geotechnical Parameter Test Results.....81
Table 4.5	Result of Calculated Density Values and Model Resistivity Values at Designated Location.....87
Table 4.6	Detailed of ERT Model Information Characteristics.....90
Table 4.7	Summarised Geotechnical Properties of The Four Tested Soils.....90
Table 4.8	Shows the Test Samples Shear Stress and Normal Stress for Test A, B, C & D.....98
Table 4.9	Summarized Results of Grading and Empirically Calculated Hydraulic Conductivities from Particle Size Distribution Analysis.....108
Table 4.10	Analysed Results of the Particle Size Distribution of the Collected Soil Samples.....111
Table 4.11	Shows the Percentage Deviation Error Computed for the EDHC and LDHC.....119
Table 4.12	Show borehole depths, soil resistivity values, and empirically derived hydraulic conductivity (EDHC) values from Beyer, Kozeny-Carman and Slitcher formulae.....120



## LIST OF FIGURES

	<b>Page</b>
Figure 2.1	Ohm’s Law on a Current passing through a Conductor of Length, $L$ and Cross-Sectional Area, $A$ .....17
Figure 2.2	The Current Flow and Equipotential Distribution in a Homogeneous and Half Space Medium, (a) A Single Point Current Source, (b) Four Electrode Method.....18
Figure 2.3	The Conventional Four Electrodes Arrangement for the Subsurface Resistivity Measurement.....19
Figure 2.4	Shows Wenner-Schlumberger Array System with its Corresponding Geometric Factors, $K$ , the Electrode Spacing $a$ , and the Spacing Integer Factor, $n$ .....20
Figure 2.5	A Conventional Collinear Four Electrode Arrangement to Measure the Subsurface Resistivity.....22
Figure 2.6	The ALERT-ME System Developed by BGS.....25
Figure 2.7	Time-Lapse 2-D Resistivity Sections.....26
Figure 2.8	Build-up of Moisture Prior to Slope Failure Inferred from 2-D ERT.....27
Figure 2.9	A Schematic Diagram Illustrating the Approach of Water Content Mapping Using ERT.....27
Figure 2.10	Schematic representation of soil phases.....28
Figure 2.11	Schematic Diagram of Constant Head Permeability Test.....32
Figure 2.12	Schematic Diagram of Falling Head Permeability Test.....33
Figure 2.13	A Typical Particle Size Distribution Curve.....34
Figure 2.14	A Hypothetical Block of Weathered Rock on a Slope.....38
Figure 2.15	A Typical Rock Profile.....39
Figure 2.16	A Typical Weathering Profile in the Peninsular Malaysia.....42
Figure 3.1	Structural relief map of Penang Island district .....53
Figure 3.2	Map of the study site showing relief of the Study Location .....55

Figure 3.3	Shallow landslides photo images (A-E) with the red dotted lines showing the previous landslides area extent in the study location.....	56
Figure 3.4	Geological Map of Penang Island showing the study site location in the medium to coarse grained Biotite Granite .....	58
Figure 3.5	The Multidisciplinary Workflow.....	59
Figure 3.6	Fieldwork Data Acquisition: Fieldwork data acquisition materials ABEM SAS 4000 Terrameter connected to Selector ES 1064 and cables with electrodes.....	61
Figure 3.7	(a) Calibrated Cylindrical Steel Core Cutter Containers, (b) Collection of Undisturbed Soil Samples and carefully wrapped with Cellophane Paper for Density Determination.....	65
Figure 3.8	(a) Constant Head Permeability Test, and (b) Falling Head Permeability Test experimental set up.....	66
Figure 3.9	(a) Components of the Shear Box (b) The Direct Shear Apparatus...	68
Figure 3.10	Map of soil sampling locations for the hydrogeological assessment.....	69
Figure 3.11	Particle Size Distribution Analysis Apparatus (A) A Mechanical Shaker for Sieving Soil Samples, (B) An Oven for Drying Soil Samples, (C) A Chemical Weighing Balance for Weighing Soil Samples.....	70
Figure 3.12	The Complete Flow Chart Diagram of the Research Methodology....	72
Figure 4.1	ERT Model Interpretation of the acquired data at different dates using Wenner-Schlumberger array, (A & B) profiles in east-west direction on 13 <sup>th</sup> Nov. 2019, (C & D) profiles in east-west direction on 22 <sup>nd</sup> Jan. 2020 and (E & F) profiles in north-south directions on 23 <sup>rd</sup> Jan. 2020.....	78
Figure 4.2	Typical Particle Size Distribution Curves in The Study Site.....	84
Figure 4.3	Relationship between Density and Resistivity in the Study Location.	87
Figure 4.4	The Arrangement of Model Blocks and Apparent Resistivity Datum Points.....	90
Figure 4.5	Interpreted ERT model result for profile G showing model resistivity with topography.....	91
Figure 4.6	Interpreted ERT model result for profile H showing model resistivity with topography.....	92

Figure 4.7	The stress-strain relationship for Test A, B, C and D with Soil moisture contents.....	95
Figure 4.8	Vertical Strain vs Horizontal Displacement curves: Direct Shear Test for Test A, B, C and D Soil Samples show that lower percentage of Silt and Clay content were more dilative as seen in the Test C and D but Test A and B with higher percentage of Silt and Clay content show contraction of the tested soil samples.....	97
Figure 4.9	Direct Shear Test for Test A, B, C and D Soils Failure Envelope on Shear Stress-Normal Stress Plane with Test C having lowest angle of internal friction of $30^{\circ}$ .....	99
Figure 4.10	Shear Stress-Normal Stress Plane Showing an Increase in Cohesion and Monotonic Behaviour of the Tested Soils.....	100
Figure 4.11	An old soil pipes with crack roof filled with dry leaves.....	103
Figure 4.12	Interpreted Inverted ERT Model from the Study Site.....	104
Figure 4.13	Soil piping in the study site (A)-(C) soil piping with a portion of its roof retained, (D) soil piping with total roof collapsed.....	106
Figure 4.14	Gullies developed from the soil piping (A-B) Pond reservoir for falling water in the gully developed from soil piping, (C-F) Zone of rapid water movement through the gullies that can create slope .....	107
Figure 4.15	The moisture content maps for 0-0.25 m depth and 0.25-0.50 m depth.....	110
Figure 4.16	Typical Characteristic Particle Size Distribution Curve from the Study Site.....	112
Figure 4.17	Map showing the empirically computed hydraulic conductivity for Beyer formula within 0-0.25 m and 0.25-0.50 m depth.....	114
Figure 4.18	Map showing the empirically computed hydraulic conductivity for Kozeny-Carman formula within 0-0.25 m and 0.25-0.50 m depth.....	115
Figure 4.19	Map showing the empirically computed hydraulic conductivity for Slitcher formula within 0-0.25 m and 0.25-0.50 m depth.....	116
Figure 4.20	Relationship between soil resistivity and hydraulic conductivity estimated from Beyer formular.....	121
Figure 4.21	Relationship between soil resistivity and hydraulic conductivity estimated from Kozeny-Carman formular.....	122

Figure 4.22 Relationship between soil resistivity and hydraulic conductivity estimated from Slitcher formular.....122

## LIST OF ABBREVIATIONS

1-D	One Dimensional
2-D	Two Dimensional
ALERT-ME	Automated Time-Lapse Electrical Resistivity Tomography
AR	Apparent Resistivity
BGS	British Geological Society
BS	British Standard
CST	Constant Separation Traversing
EDHC	Empirically Derived Hydraulic Conductivity
ERT	Electrical Resistivity Tomography
ES 464	Electrode Selector 1064
GPRS	General Packet Radio Service
HM	Horizontal Mapping
HP	Horizontal Profiling
LDHC	Laboratory Determined Hydraulic Conductivity
LP	Location Point
NPP	North Penang Pluton
PC	Personal Computer
PSD	Particle Size Distribution
RMS	Root Mean Square
SPP	South Penang Pluton
VES	Vertical Electrical Soundings

## LIST OF SYMBOLS

%	Percentage
$c'$	Cohesion
$\tan\theta'$	Friction angle
$\rho_b$	Bulk Density
$\rho_d$	Dry Density
$\sigma'$	Normal Stress at Failure
$\tau_f$	Shear Stress at Failure
$\mu$	Dynamic Viscosity
$\rho$	Apparent Resistivity
$\rho_w$	Density of Water
$\Omega m$	Ohmmeter
$\alpha$	Proportionality
$\gamma$	Volumetric Water Content
$\pi$	Pi
$^{\circ}C$	Degree Celsius Temperature
$\phi$	Phi (Diameter)
'	Minutes
"	Seconds
<	Less Than
>	Greater Than
$\Delta h$	Head Loss
$\Delta V$	Potential Difference
$2\pi r^2$	Area of Hemisphere
$4\pi r^2$	Area of Sphere

A	Cross section Area
C	Sorting Coefficient
$C_1$ & $C_2$	Current Electrodes
$C_c$	Coefficient of Gradation
$C_u$	Coefficient of Uniformity
$D_{10}$	Diameter of 10 % finer
$D_{30}$	Diameter of 30 % finer
$D_{60}$	Diameter of 60 % finer
$d_e$	Effective Size
$D_i$	Deviation
E	East
$e$	Void Ratio
$f(n)$	Porosity Function
$g$	Acceleration due to Gravity
$g$	Gramme
$i$	Hydraulic Gradient
I	Electrical Current
$k$	Hydraulic Conductivity or Coefficient of Permeability
K	Geometric Factor
Kg	Kilogrammes
KPa	KiloPascal
L	Length
m	Metre
M	Total Mass of soil
$m(x)$	Mean Value

m/s	Metre per Second
mm	Millimetre
$M_s$	Mass of Solid Soil
$M_w$	Mass of Water
n	Porosity
N	North
$P_1$ & $P_2$	Potential Electrodes
$q$	Discharge or Rate of Flow
r	Radius
R	Resistance
$R^2$	Regression
S	South
SI	International System of Units
$S_r$	Degree of Saturation
$t$	Time
$\nu$	Kinematic Viscosity
$V_s$	Volume of Solid Soil
$V_t$	Total Volume of Soil
$V_v$	Volume of Voids
$V_w$	Volume of Water
$v$	Laminar Velocity
W	West
$W_1$	Weight of Empty Can
$W_2$	Weight of Empty Can + Wet Soil Sample
$W_3$	Weight of Empty Can + Dry Soil Sample



$w$	Gravimetric Water Content
$x_i$	Data Element

**PENCIRIAN TOMOGRAFI KEBERINTANGAN ELEKTRIK 2-DIMENSI  
GEOTEKNIK DAN ANALISA KEKONDUKSIAN HIDRAULIK KE ATAS  
TANAH BAKI GRANIT**

**ABSTRAK**

Penyelidikan ini bertujuan untuk mencirikan model Tomografi Keberintangan Elektrik (ERT) 2-D untuk perubahan dalam ketepuan tanah, menganalisis sifat geoteknikal tanah baki untuk pengesahan model ERT serta membangunkan hubungan antara keberintangan tanah dan Kekonduksian Hidraulik (HC) untuk pencirian litologi bagi penilaian dalam ketidakstabilan kecerunan. Walau bagaimanapun, hubungan antara HC dan ERT untuk penilaian pencirian litologi bagi ketidakstabilan kecerunan dalam tanah baki ini masih jarang berlaku. Sembilan (9) data ERT telah diperoleh dalam penggunaan susunatur Wenner-Schlumberger. Dua puluh sembilan (29) sampel tanah telah dikumpulkan dengan kedalaman 0–4.5m menggunakan pemotong teras silinder dan gerudi tangan untuk dianalisis secara geoteknikal dan HC. Keputusan ERT yang dianalisis menunjukkan tiga zon geologi iaitu 1–600  $\Omega\text{m}$  sebagai zon Kandungan Air Tinggi (HWC), 600–3000  $\Omega\text{m}$  sebagai zon Lapisan Lemah (WL) dan >4000  $\Omega\text{m}$  sebagai batu tongkol dan pengapung. Zon HWC dicirikan sebagai amblesan dan kemungkinan struktur kerutuhan apabila batu tongkol dan pengapung bertindih dengan zon tepu semasa hujan lebat yang berpanjangan bertindak sebagai faktor pencetus kepada ketidakstabilan dan kegagalan pada kecerunan. Model ERT menunjukkan permukaan kegelinciran di sempadan antara kandungan air tinggi dan zon lapisan lemah pada kedalaman 3-4 m. Hasil geoteknikal menunjukkan bahawa kawasan yang keberintangan relatif rendah <600  $\Omega\text{m}$  mempunyai Kandungan Kelembapan (MC)

tinggi, 30.1% dengan ketumpatan rendah,  $1176 \text{ kg/m}^3$  dan HC,  $2.02 \times 10^{-5} \text{ m/s}$  manakala kawasan keberintangan tinggi  $< 3000 \text{ } \Omega\text{m}$  mempunyai MC yang lebih rendah, 11.4% dengan ketumpatan yang agak tinggi  $1458 \text{ kg/m}^3$  dan HC  $1.34 \times 10^{-2} \text{ m/s}$ . Sifat kejuruteraan tanah mengesahkan keputusan ERT kerana sudut geseran dalaman yang paling rendah iaitu  $30^\circ$  dan jelekitan 8 KPa menunjukkan permukaan tanah runtuh yang berpotensi. Ia telah digariskan pada kedalaman 3-4 m di sempadan antara tanah berkerikil dan berkelodak. Penilaian hidrogeologi bagi Kekonduksian Hidraulik Terbitan Empirik (EDHC) menunjukkan bahawa galur  $> 2 \text{ m}$  akan membawa kepada ketidakstabilan kecerunan. Nilai Kekonduksian Hidraulik Ditetapkan Makmal (LDHC) sebanyak  $4.06 \times 10^{-5}$  dan  $5.80 \times 10^{-5} \text{ m/s}$  telah disahkan dengan keputusan EDHC kerana nilai ralat kesisihan pada peratusan yang rendah iaitu 29% dan 13% masing-masing diperoleh mengikut penganggaran EDHC daripada formula Beyer. Tambahan pula, hasil hubungan antara HC dan ERT dapat mencirikan litologi kepada media telap dan kurang telap untuk tanah berkerikil dan berkelodak masing-masing. Secara kesimpulannya, kawasan keberintangan rendah yang terdiri daripada tanah yang mempunyai nilai HC yang rendah merupakan punca utama kepada ketidakstabilan kecerunan dan bertanggungjawab terhadap pembangunan paip tanah yang turut mewujudkan ketidakstabilan kecerunan di kawasan tersebut. Akhir sekali, permukaan gelincir tanah gelongsor yang berpotensi boleh diperhatikan dan jelas berdasarkan keputusan yang dianalisis.

**CHARACTERIZATION OF 2-DIMENSIONAL ELECTRICAL  
RESISTIVITY TOMOGRAPHY, GEOTECHNICAL AND HYDRAULIC  
CONDUCTIVITY ANALYSIS IN THE GRANITIC RESIDUAL SOIL**

**ABSTRACT**

This research aims to characterise 2-D Electrical Resistivity Tomography (ERT) models for changes in soil saturation, analyse geotechnical properties of residual soil for validation of ERT models and develop a relationship between soil resistivity and Hydraulic Conductivity (HC) for lithological characterisation for slope instability assessment. However, relationship between HC and ERT for lithological characterization for slope instability assessment in this residual soil is still rare. Nine (9) ERT data were acquired using Wenner-Schlumberger array. Twenty-nine (29) soil samples were collected within 0–4.5 m depth using cylindrical core cutter and hand auger dug borehole for geotechnical and HC analysis. Analyzed ERT results revealed three geological zones of 1–600  $\Omega\text{m}$  as High-Water Content (HWC) zones, 600–3000  $\Omega\text{m}$  as Weak Layer (WL) zones and  $>4000 \Omega\text{m}$  as boulders and floaters. The HWC zones were characterized by subsidence and possible collapsed structures of boulders and floaters overlies saturated zones during prolonged heavy rainfall act as triggering factors for slope instability and failure. The ERT models revealed a slip surface at the boundary between high-water content and weak layer zones within 3–4 m depth. Geotechnical results show that relatively low-resistivity  $<600 \Omega\text{m}$  areas have high Moisture Content (MC), 30.1% with low density, 1176  $\text{kg/m}^3$  and HC,  $2.02 \times 10^{-5} \text{ m/s}$  whereas high resistivity  $<3000 \Omega\text{m}$  areas have lower MC, 11.4% with relatively high

density  $1458 \text{ kg/m}^3$  and HC  $1.34 \times 10^{-2} \text{ m/s}$ . The soil engineering properties confirmed the ERT result because the lowest angle of internal friction of  $30^\circ$  and cohesion of 8 KPa indicate a potential landslide slip surface. It was delineated within 3-4 m depth at boundary between gravelly and silty soils. Hydrogeological assessment of Empirically Derived Hydraulic Conductivity (EDHC) revealed that gullies of  $>2 \text{ m}$  will lead to slope instability. Laboratory Determined Hydraulic Conductivity (LDHC) values of  $4.06 \times 10^{-5}$  and  $5.80 \times 10^{-5} \text{ m/s}$  were validated with the EDHC results because low percentage deviation errors values of 29% and 13% were obtained respectively for the EDHC estimator from Beyer formula. Furthermore, the results of relationship between HC and ERT were able to characterize the lithology into permeable and less-permeable media for gravelly and silty soils respectively. Conclusively, low-resistivity areas are composed of low HC soils which were precursors to slope instability and responsible for the development of soil piping that creates slope instability in the area. Lastly, a potential landslide slip surface is observable and evident based on the analysed results.

## CHAPTER 1

### INTRODUCTION

#### 1.1 Overview of background

There are great concerns around the world over the years on the occurrences of damaging landslides (De Vita et al., 2018; Froude & Petley, 2018; Hojat et al., 2019). Slope movement events that resulted in landslide have wrecked severe havoc and damage to lives and infrastructures with estimated loss of several billions of dollar across the world (Bordoni et al., 2018; Di Traglia et al., 2018; Kirschbaum et al., 2020; Moragues et al., 2019; Soto et al., 2017; Tomás et al., 2018; Wang et al., 2017; Yang et al., 2019). The impact of damages caused to lives and infrastructure as well as mitigation and management of this natural hazard has been the subject of research for decades (Abidin et al., 2017; Pasierb et al., 2019). In Penang Island, Malaysia, urbanisation has led to expansion and building of structures into slope areas that are prone to slope instability, which needs to be investigated. These slope instabilities occurred as shallow landslides within the residual soil of weathered granitic basement triggered by heavy rainfall. With a daily annual average rainfall as high as 6470 mm, maximum high temperature of 35°C and daily relative humidity as high as 96.8% in some cases (Ahmad et al., 2006; Ali et al., 2011). These climatic factors are responsible for rapid weathering of the granitic rocks which makes the slope to be potentially unstable resulting in failure with shallow landslide occurrences in Balik Pulau and Paya Terubong axis. In this study, the climatic data was obtained from the Penang International Airport, which was about 6 km away. The average annual rainfall of 1740.2 mm, mean annual temperature of 28.7 °C, mean annual relative humidity of 76.2 % were observed in the study site in the year 2019.

Seasonal change of wet and dry in Peninsula Malaysia subjects the rocks to undergo weathering that help to breakdown the rock into smaller particles called residual soil through physical and chemical processes (Eppes & Keanini, 2017; Sajinkumar et al., 2011). Residual soil types derived from decomposed granite show the highest degree of weathering near the ground surface which decreases in intensity to essentially unweathered materials at depth. Infiltration of rainwater into the ground increases the soil saturation and pore water pressures which are trigger to landslide (Askarinejad et al., 2018). Friable soils on hill slope areas are prone to rapid infiltration during heavy rainfall. The loose soil materials undergo rapid infiltration during heavy rainfall and become saturated. The rainwater which flows down through the soils displaces air that fill the void spaces in the vadose zone. This water occupying the pore spaces increases the pore pressure in the unsaturated zone and creates unstable areas with locally elevated pore water pressure (Reid, 1997; Sultan et al., 2001). The increase in pore-water pressure in the soils induces slope instability and triggers off landslides in some cases. Cases of slope instabilities are common occurrences as reported in several publications (Di Traglia et al., 2018; Moragues et al., 2019; Sidle & Bogaard, 2016; Soto et al., 2017; Tomás et al., 2018). According to the available data on global catalog of landslides, with Multi-Satellite Precipitation Analysis records, have shown that majority of landslide occurrences over the world were triggered by extreme rainfall events (Kirschbaum et al., 2015). Hojat et al., (2019) have also shown that landslide-prone slope becomes unstable at zones where the water saturation exceeds 45% and they observed that slope instability could occur at the boundaries between areas with different water saturations. This changes in water saturations and slope geometry are the main factors that induces slope instability (Tang et al., 2018) in the presence of discontinuities such as -faults, fractures, beddings etc.- which are precursors to

landslide (Chalupa et al., 2018). Since, the world is experiencing heavy and extreme rainfall events because of global climate change (Kirschbaum et al., 2020). The continuous precipitation during typhoon increases slope instability around mountains which have led to severe mudflows and landslide events (Hakro & Harahap, 2015; Jeong et al., 2017; Jeong et al., 2014; Kirschbaum et al., 2020; Kumar & Rathee, 2017; Sidle & Bogaard, 2016b). Majority of these landslides have caused a considerable loss of lives and property (Askarinejad et al., 2018; Choi & Cheung, 2013).

Conventional method of characterizing these landslides bodies is based on intrusive investigation sampling from boreholes or open pits to obtain information about the soil variability. But this method is destructive to the soil, expensive, time consuming and direct information are difficult to achieve. However, in characterizing unsaturated residual soil with high soil spatial variability, the use of geophysical technique of Electrical Resistivity Tomography (ERT) to study soil prone to landslide is very appropriate because it is fast, rapid and non-invasive (Buvat et al., 2014). ERT has been proved useful in subsurface imaging of soil to delineate slip surfaces of landslide and monitor unstable areas of instabilities in the slope (Boyle et al., 2018; Hojat et al., 2019; Ismail & Yaacob, 2018; Pasierb et al., 2019; Tomás et al., 2018; Tomecka-Suchoń et al., 2017; Whiteley et al., 2019). ERT has the advantages of non-invasive and non-destructive nature of probing the subsurface and it is relatively cheap with rapid results that are compatible with subsurface earth materials, waste pollutant and anthropogenic materials (Lech et al., 2020). Electrical resistivity is responsive to changes in the pore fluid resistivity and saturation, since the principal mode of current flow within the pore fluid of earth materials is through electrolytic process (Samouëlian et al., 2005). Therefore, ERT can conduct electric current through fluid in rock's and soil's voids and pore spaces. ERT is capable of distinguishing between



lithologies of contrasting resistivity where the cause of changes in resistivity is due to presence of clay minerals or differing porosities (Archie, 2003; Hen-Jones et al., 2017; Shevnin et al., 2007). In coarse grained (silica quartz minerals) soils with lesser voids and pore spaces through which electric current can flow may be affected by the amount of pore fluid (saturation) that will significantly influence the results of the resistivity test. The relationship between the pore fluid resistivity and saturation is fully explained by Archie Equations (Archie, 2003). But, in soil with clay minerals, soil resistivity is lower than that of granular (sands and gravels) because electric current flow is through surface conduction, a phenomenon referred to as double layer due to additional matrix conduction is caused by the movement and distribution of ions through the clay particles surfaces (Gunn et al., 2015). Hence, high amount of clay minerals in the soil is generally related to a low resistivity value (Martin, 2019; Waxman & Smits, 1968; Yamakawa et al., 2012). Therefore, an accurate interpretation of ERT data requires the integration of geological information for validation of the soil properties.

Geotechnical engineering studies of the properties of residual soil is very important for monitoring slope instability. Knowledge of engineering characteristics of residual soil may offers significant information about the slope soil shear strength parameters and its bearing capacity (Han et al., 2020; Mandisodza & Dunn, 2019; Salih, 2012; Wei et al., 2019; Wibawa et al., 2018). It has been shown that soil's shear strength parameters and stress-strain behavior are significantly affected by porosity, stress history and the bonds between soil particles (Chang & Cho, 2019; Meng & Chu, 2011). Since, engineering measures cannot always provide enough protection against the landslide occurrence, it is imperative that effective warning systems should be developed to avoid slope disasters caused by severe weather (Chien et al., 2015). Therefore, understanding the hydrogeology of the residual soil is required for

monitoring and predicting slope instability to provide early warning to be able to avert impending landslide catastrophic events. Hence, hydraulic conductivity, which is the ease at which water flow through the soils, plays a major role in the developments of slope instability. It is responsible for the initiation of soil piping which creates gully erosion that causes slope instability especially in friable soils with low cohesion and high hydraulic conductivity because high hydraulic conductivity slope soil causes rapid increase in pore-water pressure during heavy rainfall leading to increase slope instability (Mukhilsin & Taha, 2010). Several studies of the impact of hydraulic conductivity on slope instabilities have been published, which were based on its hydromechanical contributions to hillslope hydrological process (Bernatek-Jakiel & Poesen, 2018; Jones, 2010; Okeke & Wang, 2016; Schneider, 2014; Vardon et al., 2016; Yeh et al., 2015).

Slope instability in weathered igneous rock has long been the subject of research over the years. However, research work on the impact of the subsurface changes in soil saturation in gravelly sand soil within the unsaturated zone of the residual soil is rare. Therefore, this study was focussed on the characterisation of 2 – Dimensional (2-D) ERT models, geotechnical properties and hydraulic conductivity analysis in residual soil for slope instability assessment.

## **1.2 Problem statement**

Slope instabilities are major problems encountered in the hill slope around the world. These slope instabilities are often landslides triggered by rainfall water accumulated within the unsaturated zone resulting in a perched saturated zone of the part of slope soil which can weaken a section of the slope. Urbanisation in Penang Island has led to expansion and building of structures into slope areas that are prone to slope instability caused by shallow landslides and soil internal erosion due to poor drainage of

rainwater and low cohesion of friable soils. Its occurrences has resulted in loss of lives and properties due to devastating destructive capacity. For example, heavy rainfall triggered landslide on a residual/deeply weathered soil on the 19<sup>th</sup> of October 2018 killing nine (9) construction workers located in a temporary accommodation at the foot of a slope at Jalan Bukit Kukus in Gorge town, Penang Island. Therefore, it is important to accurately map this zone of groundwater accumulation. However, response to most geohazard occurrences around the world is responsive rather than proactive. In this study, concerted efforts are made to characterise and analyse this slope instability using geophysical, geotechnical and hydrogeological methods for monitoring and assessment of slope instability occurrence to save lives and properties that can be lost to the devastation effect of its occurrences. In a recent study, Hojat et al., (2019) have used geophysical technique of ERT in the laboratory to characterize the subsurface of a landslide and observed that slope instability occurs zones where the water saturation exceeds 45% especially at the boundaries between areas with different water saturations. Seasonal effects on geophysical – geotechnical relationships with their implications using ERT for monitoring of slope instability were presented by Hen-Jones et al., (2017). Furthermore, Han et al., (2020) have shown that soil water content influences the soil shear strength parameters of soil such as, angle of internal friction and cohesion because as soil water content increases the soil shear strength reduces, consequently, causing a reduction in the soil stability. Therefore, the evaluation of these engineering properties of the soil is crucial and of great importance in slope instability studies (Wei et al., 2019). Hence, the analysis of slope-related problems requires the integration of engineering properties of the soil to obtain a considerable result for monitoring of slope instability in unstable slopes. The present study integrated hydrogeological and geotechnical approach to evaluate and

calibrate the ERT models obtain from geophysical measurements on the slope soils for monitoring of slope instability within the residual soil.

### **1.3 Aim and objectives**

The aim of the study is to analyse hydraulic conductivity and geotechnical properties of soil to assist the characterisation of 2-D ERT for monitoring of slope instability in the granitic residual soil.

#### **Specific objectives are:**

- (i) to characterise and analyse 2-D ERT models for changes in soil saturation and detect subsurface soil piping that can induce slope instability.
- (ii) to analyse geotechnical properties of residual soil for validation of 2-D ERT models.
- (iii) to develop a relationship between formation electrical resistivity and hydraulic conductivity for lithological characterisation and hydrogeological assessment of hydraulic conductivity of poor drainage conditions inducing slope instability.

### **1.4 Scope of the study**

Penang island is located in the northern part of Peninsula Malaysia. It is centrally occupied by Penang hills of granitic origin and it is rapidly becoming a major metropolitan city with the influx of tourist and increase in construction and industrial activities leading to expansion and building of infrastructure around slope area. With a daily maximum high temperature of 35°C, annual average rainfall as high as 647 cm and daily relative humidity as high as 96.8% in some cases (Ahmad et al., 2006; Ali et al., 2011). These climatic factors are responsible for rapid weathering of the granitic

rocks which makes the slope to be potentially unstable resulting in failure with shallow landslide occurrences in Balik Pulau and Paya Terubong axis.

The study site selected for this research work is within the Paya Terubong area where recent activities of slope failures had occurred. The study was conducted on an area of 41 m by 50 m (2050 m<sup>2</sup>) and it was focussed within the residual soil of weathered granitic basement, which is widely affected by shallow landslides during prolonged heavy rainfall in the area. This study analysed ERT model to monitor the subsurface water accumulation, saturation and movement in the unsaturated residual soil, which causes abnormal pore water pressure built up that could induce slope instability. It also determines soil engineering properties responsible for slope instability. The subsurface analysis and monitoring of the slope instability in the residual soil is limited to the 2-D, ERT while the soil engineering properties determination help to calibrate the results of the ERT model analysis. Also, a relationship was developed between hydraulic conductivity and soil resistivity for lithological characterisation and hydrogeological assessment of hydraulic conductivity of poor drainage conditions. The ERT investigation was conducted using Wenner-Schlumberger array configuration with a survey profile of 60 m length and 1.5 m electrode spacing through electrical resistivity soundings but the procedure for the determination of soil engineering properties are largely based on laboratory tests and experiments. Soil sampling was the basic procedure for obtaining hydraulic conductivity which was analysed empirically and in the laboratory. However, this procedure for the slope instability monitoring in the residual soil could be implemented in a different geological setting.

The layout of the survey site limits the depth of investigation because of the restriction of accessibility by manmade structures such as shrines and fences and slope morphology. The ERT survey profile electrode spacing interval of 1.5 m help to obtain

detail image of the subsurface so that it could not miss some traces of water accumulation materials or structures and fractures in the interpretation of the analysed ERT models.

### **1.5 Significant of the study**

Prolong heavy rainfall is increasingly inducing slope instabilities on the high-risk hills of weathered granitic basement in Penang Island. These slope instabilities are spatially controlled with changes in geotechnical properties of the slope soils. The rainwater which flows down through these slope soils displaces air that fill the void spaces in the vadose zone. This water occupying the pore spaces increases the pore pressure in the unsaturated zone and creates unstable areas with locally elevated pore water pressure (Reid, 1997; Sultan et al., 2001). But, subsurface water movement depends on soil hydraulic conductivity, which is the ease of water or fluid flow through the pore spaces of the soil. This movement of soil water or fluid through the pore spaces depend on the type of soils, it is higher in coarse grained soil (sand) than in fine grained soil (silt and clay) (Saravanan et al., 2019). Seasonal changes in soil water content affects the hydraulic conductivity of the soil (Hu et al., 2012). Therefore, a good knowledge of soil hydraulic conductivity is vital for slope instability assessment.

Also, geophysical technique of electrical resistivity tomography has been widely used for slope instability assessment because it is responsive to changes in pore water or fluid of soil or rock. But, geophysical methods involve the acquisition of data, which are sets of measurements from a model and it can be used to reconstruct an estimated model (Snieder & Trampert, 1999). The true model is unique, but the estimated model is non-unique. This problem of non-uniqueness is common to most geophysical models (Vasco, 2007). Therefore, geophysical interpretation requires integration of the geological information for the validation of the estimated model to overcome the

problem of non-uniqueness associated with geophysical model (Loke et al., 2013; Perrone et al., 2014). Hence, research work on monitoring and assessment of slope instability using the geotechnical properties of soil to validate the result of geophysical model because of the problem of non-uniqueness solutions has not been fully demonstrated. Previous published works available on slope instabilities have used integration of geophysical and geotechnical techniques to show that landslides were triggered by heavy rainfall due to presence of clay (Dahlin et al., 2013; Hughes et al., 2013; Ismail & Yaacob, 2018; Jamalludin et al., 2014; Pasierb et al., 2019; Soto et al., 2017). However, research work on the impact of hydrogeology on slope instability by relating hydraulic conductivity to the soil resistivity for characterization of changes in water content of residual soil for slope instability assessment is rare.

## **1.6 Thesis structure**

The thesis is organised in five chapters. Following introduction chapter is chapter 2, which presents the theoretical background and basis for the work contained in the subsequent chapters. The review of the basic principles of the electrical resistivity technique, especially its use in monitoring water accumulation zones in landslide studies is given. The principles of geotechnical measurement techniques of engineering properties of soils are discussed.

Chapter 3 presents the materials and methods which include location, climate and geology of the chosen site. The procedures of data acquisition, analysis and interpretation are discussed. Chapter 4 presents the experimental and investigation results and discussion of results of the outcomes of the methods described in Chapter 3. Chapter 5 summarizes the significant findings and conclusion of the research. It also provides useful recommendation for future work.

## CHAPTER 2

### LITERATURE REVIEW

#### 2.1 Introduction

Electrical Resistivity Tomography, a technique of electrical resistivity method, provides a non-invasive, quick and relatively cheap subsurface imaging of the unstable slopes of residual soil. Slope instability is prevalent in the residual soil of granitic basement especially in the humid climate around the world. A wide range of techniques has been developed to study slope instability in areas characterized by complex geological setting from several published research works (Baharuddin et al., 2016; Chalupa et al., 2018; Di Traglia et al., 2018; Pasierb et al., 2019). It has been observed that over the last two decade the technological improvements in the field-data acquisition systems and the development of novel algorithms for tomographic inversions have made ERT more suitable for studying landslide areas, with a particular attention to the rotational, translational and earth-flow slides (Perrone et al., 2014). However, this technique has both advantages and disadvantages which have been discussed in section 2.2.2. The drawbacks can be improved with the geotechnical investigation and hydrogeological assessment of hydraulic conductivity of the soil in the laboratory and on the field. Analysis of both the geotechnical properties and hydraulic conductivity of the residual soil can assist in the characterization of the ERT models in slope instability monitoring in evaluating soil water content changes (Hübner et al., 2015) and correlating parameters such as dry density (Bery & Saad, 2012; Vincent et al., 2017), hydraulic conductivity (Bernatek-Jakiel & Poesen, 2018; Vardon et al., 2016; Yeh & Tsai, 2018) and shear strength (Han et al., 2020; Mandisodza & Dunn, 2019; Wibawa et al., 2018).



## 2.2 Previous studies

Previous work undertaken on slope instability using geophysical technique or combination of both geophysical and geotechnical techniques by various researchers have been documented (Giocoli et al., 2015; Han et al., 2020; Hen-Jones et al., 2017; Hübner et al., 2015; Pasierb et al., 2019; Popescu, 2014). Giocoli, *et al.*, (2015) have used a multidisciplinary approach based on the integration of different techniques of geophysical surveys, aerial photos, geological field surveys and borehole data to investigate landslide in an area located in the Basilicata Region, southern Italy. The landslide was located in a steep slope encased stream in a narrow and deep land incisions with abrupt tectonic changes and lithology variations. It is an area that have been subjected to hydrological and geological instability resulting in several active landslide activities. Geophysical data acquisition were conducted using Wenner-Schlumberger electrode array with survey length of 940 m and electrode spacing of 20 m to achieve a depth of investigation of 150 m depth. The ERT was able to characterize the geometry of the landslide, locate the sliding surface and estimate the thickness of the landslide body. Likewise, Popescu, *et al.*, (2014) also used ERT to investigate the reactivation of the old landslide structure of active slide around Buzad village. The ERT data were obtained using Wenner array in time lapsed in years 2007, 2012, and 2014 with survey length of 100 m and penetration depth of 15 m in 2007 and 2012. The result of ERT measurements revealed information about the geometry, characteristics and the depth extension of landslide body and indicated zones of high-water content and clay content which triggers the landslide body. Therefore, ERT was able to delineate the high-water content responsible for the reactivation of the landslide. In another development, Chambers, *et al.*, (2014) have also used installed ERT arrays to monitor temporal variations of electrical resistivity within slopes,

thereby evaluating variations in soil moisture of the slope. Soil water variations in the soil within slopes induce instability which were monitored with surface ERT measurements to determine water content and the results showed a strong correlation with the hydrometric data (Hubner, *et al.*, 2015). Recent studies on landslides have shown that ERT is suitable to monitor soil water content variations induced by rainfalls among other methods such as seismic refraction, seismic reflection, self-potential and ground penetrating radar (Boyle *et al.*, 2018; Hojat *et al.*, 2019; Whiteley *et al.*, 2019). Hojat *et al.*, (2019) applied time-lapse ERT for monitoring a rainfall-triggered landslide simulator in the laboratory. They monitor rainwater infiltration through landslide body using time-domain reflectometry to obtain volumetric water content and calculated water saturation to improve the understanding of precursors of failure. Hen-Jones *et al.*, (2017) have used geophysical and geotechnical sensors to monitor groundwater conditions due to seasonal changes with ERT to determine the relationship between resistivity, shear strength, suction and water content in monitoring of slope instability. ERT is applied in order to characterize lithostratigraphic sequences and geometry of the sliding body, identifying the sliding surfaces between the slide materials and underlying bedrock and location of high-water content areas or zones (Pasierb *et al.*, 2019; Tomecka-Suchoń *et al.*, 2017). Likewise, Pasierb *et al.*, (2019) used a combination of geophysical and geotechnical methods which include ERT, cone penetration testing, drilling and laboratory test to evaluate the condition of landslide and analyzing how different saturations of soil influence the stability of landslide. Consequently, an integrated approach of geophysical, geotechnical and remote sensing techniques was used by Merritt *et al.*, (2014) to investigate an active and complex landslide system in instability prone Lias Mudrocks of North Yorkshire, UK. Light Detection and Ranging (LiDAR) technique

was used to generate 3D model of the landscape to produce Digital Elevation Model (DEM). ERT was carried out using dipole-dipole array configuration and borehole data were collected for geotechnical testing. The ERT result was able to volumetrically characterize the subsurface to achieve a detailed understanding of the structure and lithology of the complex landslide system which cannot be achieved with the remote sensed data or geotechnical data alone. Furthermore, Han et al., (2020) have shown that soil water content influences the soil shear strength parameters of soil such as, angle of internal friction and cohesion because as soil water content increases the soil shear strength reduces, consequently, causing a reduction in the soil stability. Therefore, the evaluation of these engineering properties of the soil is crucial for ERT validation and of great importance in slope instability studies (Wei et al., 2019).

In Peninsula Malaysia, both shallow and deep landslides are common occurrence that are usually influenced by weathering of the granitic rocks. The nature of failure mechanisms generated in the weathering profile of the rocks are controlled by weathered materials and its structure (Ahmad et al., 2006). Most of these landslides occur after few hours of continuous heavy rainfall events in the months of October to January (Jamalludin et al., 2014). The intense and extreme heavy rainfall cause rapid infiltration that saturate the residual soil of the weathered granitic rock which triggers the landslides in most cases. Yahaya et al., (2019) have given an insight on emerging issue on landslides occurrence in Penang Island where they identified climate change as the cause of increase occurrences of the climate related geohazard. These landslides have been studied using 2-D ERT and other techniques as reported by several researchers (Abidin et al., 2017; Ghazali et al., 2013; Ismail & Yaacob, 2018; Muztaza, Ghafar, et al., 2018). Ismail & Yaacob, (2018) have applied ERT for slope failure investigation in Bukit Setiawangsa, Kuala Lumpur, Malaysia. They use Schlumberger

array, with survey length and electrode spacing of 100 m & 200 m and 2.5 m & 5.0 m respectively, for the 2-D ERT acquisition and obtained engineering properties of soil from boreholes. The laboratory derived properties – moisture content, soil hardness and Soil Penetration Test N-values – were carried out for comparison to develop a relationship between resistivity and engineering properties of soil. Their findings revealed a low resistivity zone where there is percolation of water in a permeable soil believed to be a slip surface. Abidin et al., (2017) have carried out an assessment of shallow landslide using 2-D ERT and boreholes data at the lake area in Terrengganu, Malaysia. The study was conducted using Schlumberger array system with survey length of 180 m and 3 m electrode spacing to image the subsurface geological structure and rock discontinuity associated with the low resistivity anomaly. They observed that a combination of heavy rainfall and weakness geologic materials are the major trigger factor of the failed slope. Muztaza et al., (2018) conducted 2-D resistivity survey using pole-dipole array configuration for slope failure evaluation and landslide investigation in Selangor, Malaysia. The study delineates the geology of the subsurface based on the scale of resistivity values and concluded that saturated zones, highly weathered zone and boulders were the triggering factors of the slope failure. Ghazali et al., (2013) have studied the effectiveness of ERT survey for the detection of a debris flow with water conducting zone at KM 9, Frasers Hill Gap Road (FT 148), Fraser Hill, Pahang Malaysia. The study area consists of granitic rocks that are prone to repeated slope failures with debris flows. They conducted 2-D resistivity survey parallel and perpendicular to the slope failure using Wenner array configuration with survey length of 200 m and estimated depth of penetration of about 20 to 30 m. Their findings revealed an existence of low resistivity zones which is highly fractured and water

conducting in the granite body. The shallow fractured body is above the water saturated zone which is unstable zone.

These previous studies have revealed the potential of ERT in slope instability assessment especially landslide investigation. Some of the published research works have been conducted in the laboratory while others have conducted under natural conditions to characterize water content change for slope instability assessment. Besides ERT technique other methods such as geotechnical, seismic and remote sensing have been frequently applied to study slope instability. However, the use of the relationship hydraulic conductivity to electrical resistivity for slope instability assessment is rare.

### **2.3 Review of the electrical resistivity method**

Electrical resistivity method is a physical tool used to measure resistivity of the earth materials both solid rock and weathered products. Electrical resistivity of earth materials can be defined as the resistance,  $R$ , of a resistive material is directly proportional to the length,  $L$ , of the material and inversely proportional to the cross-sectional area,  $A$  (Reynolds, 1997).

#### **2.3.1 Basic theory of electrical resistivity**

The procedure for data acquisition involves the injection of electrical current ( $I$ ), generated from a battery into the ground using four co-linear electrodes inserted into the ground consisting of two current electrodes and two potential electrodes for measuring the potential difference ( $\Delta V$ ). If we consider a current flow,  $I$ , in a cylinder of length,  $L$ , the resistance,  $R$ , of the material is directly proportional to the length of the resistive material and inversely proportional to the cross-sectional area,  $A$  (**Fig. 2.1**) (Reynolds, 1997).

$$R \propto \frac{L}{A} \quad (2.1)$$

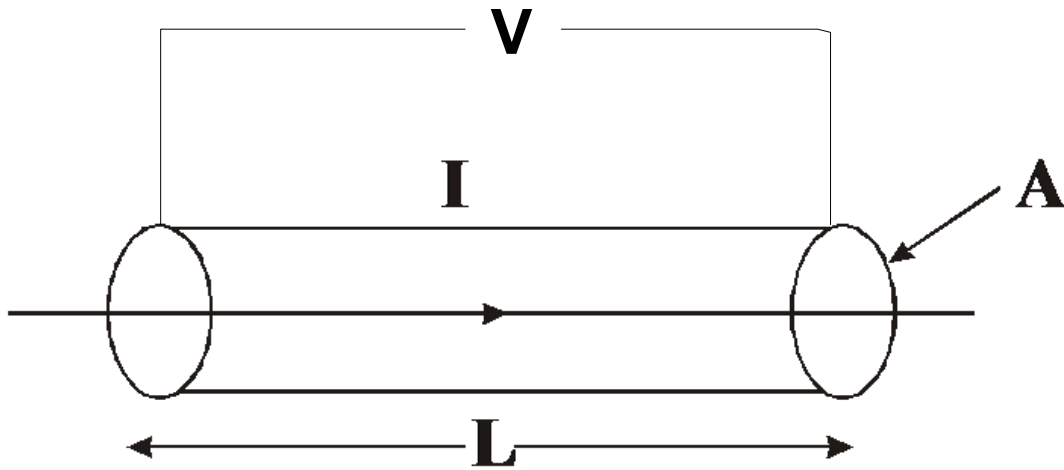


Fig. 2.1 Ohm's law on a current passing through a conductor of length,  $L$  and cross-sectional area,  $A$ .

Then,

$$R = \rho \frac{L}{A} \quad (2.2)$$

Where resistivity,  $\rho$ , is the constant of proportionality, resistance,  $R$ , length,  $L$  and cross-sectional area,  $A$  in equation (2.2).

$$R = \frac{\Delta V}{I} \quad (2.3)$$

Equation (2.3) from ohm's law,  $\Delta V = IR$ , is the potential difference **Fig. 2.1**

Substituting for  $R$  in equations (2.2) & (2.3),

$$\frac{\Delta V}{I} = \rho \frac{L}{A} \quad (2.4)$$

Then,  $\rho$ , is given as

$$\rho = \frac{\Delta V}{I} \times \frac{A}{L} \quad (2.5)$$

Equation (2.5) can be used to determine resistivity of any homogeneous or isotropic medium provided the geometry is simple e.g., Cylinders, loops, parallel pipes etc.

For an infinite homogeneous half space medium like the surface of the earth with a current electrode point source on the surface the current travels radially away from the point source and the lines of electrical potential are hemispherical about the point (**Fig.**

2.2). Therefore, the resistance at any point from the source within the medium can be calculated by determining the radius,  $r$ , from the source and the surface area of the resulting equipotential surface,  $A$ , for a sphere (Hassan, 2014).

$$A = 4\pi r^2 \quad (2.6)$$

But for hemispherical, equation (2.6) becomes

$$A = 2\pi r^2 \quad (2.7)$$

The resistance  $R$ , in equation (2.2) can be rewritten as follows

$$R = \frac{\rho L}{A} = \rho \left( \frac{r}{2\pi r^2} \right) = \frac{\rho}{2\pi r} \quad (2.8)$$

The potential due to a single current source at the surface of the earth a distance,  $r$ , away is given by ohm's law.

$$V = IR = I \left( \frac{\rho}{2\pi r} \right) = \frac{I\rho}{2\pi r} \quad (2.9)$$

Equation (2.9) is the particular equation used in electrical resistivity method, where  $\rho$  is the true resistivity. If the medium is not homogeneous,  $\rho$ , becomes apparent resistivity,  $\rho_a$  (Keller & Frischknecht, 1966).

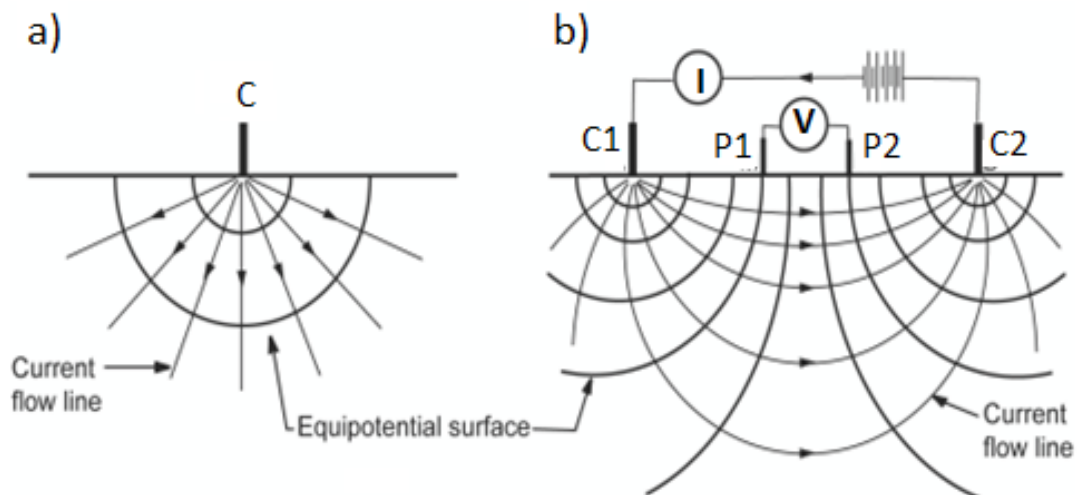


Fig. 2.2 The current flow and equipotential distribution in a homogeneous and half space medium, (a) a single point current source, (b) four electrodes method.

Electrical Resistivity is measured in the field using four co-linear electrodes inserted into the ground consisting of two current electrodes (C1 and C2) and two potential electrodes (P1 and P2) (**Fig. 2.3**).

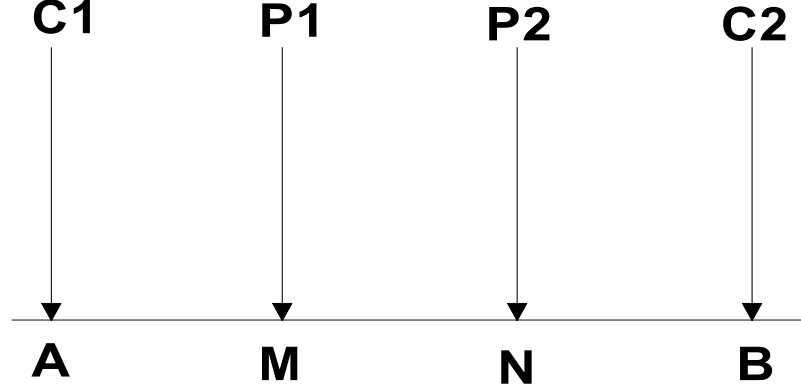


Fig. 2.3 The conventional four electrodes arrangement for the subsurface resistivity measurement.

Consider the above diagram the potential difference between P1 and P2 is given as

$$\Delta V = V_M^{AB} - V_N^{AB} \quad (2.10)$$

The potential at M due to A and B is, recall from equation (2.9),

$$V_M^{AB} = \frac{I\rho}{2\pi} \left( \frac{1}{AM} - \frac{1}{MB} \right) \quad (2.11)$$

Where,  $AM = r_1$  and  $MB = r_2$

$$V_M^{AB} = \frac{I\rho}{2\pi} \left( \frac{1}{r_1} - \frac{1}{r_2} \right) \quad (2.12)$$

The potential at N due to A and B is, recall from equation (2.9),

$$V_N^{AB} = \frac{I\rho}{2\pi} \left( \frac{1}{AN} - \frac{1}{NB} \right) \quad (2.13)$$

Where,  $AN = r_3$  and  $NB = r_4$

$$V_N^{AB} = \frac{I\rho}{2\pi} \left( \frac{1}{r_3} - \frac{1}{r_4} \right) \quad (2.14)$$

Therefore, the potential difference,  $\Delta V$ , between M and N in equation (2.10) can be expressed as

$$\Delta V = V_M^{AB} - V_N^{AB} = \frac{I\rho}{2\pi} \left( \frac{1}{r_1} - \frac{1}{r_2} \right) - \left( \frac{1}{r_3} - \frac{1}{r_4} \right) \quad (2.15)$$





So, equation (2.18) is the general form for calculating the resistivity of any electrode array system. **Fig. 2.4** shows common arrays with their geometric factor and electrode spacing.

### **2.3.2 Data acquisition**

The traditional 1-Dimensional (1-D), 2-Dimensional (2-D), 3-Dimensional (3-D) and 4-Dimensional (4-D) methods were the commonly used data acquisition for the collection of resistivity data in the field or laboratory.

#### **2.3.2a Traditional 1-D resistivity method.**

The resistivity method was first discovered in the 1920 from the work of the Schlumberger brothers. It was used for qualitative interpretation of wireline logs to conventional sounding surveys (Koefoed, 1979). In the sounding method of Koefoed (1979), the centre point of the electrodes array is fixed, while the spacing between the electrodes is increased to obtain information about the deeper section of the subsurface. This method consists of four electrodes resistivity system (**Fig. 2.5**) with a resistivity meter, four metal stakes (electrodes) and cables to connect the electrodes to the resistivity meter (Hassan, 2014). Data are acquired using Vertical Electrical Soundings (VES), Horizontal Profiling (HP) or Constant Separation Traversing (CST) and Horizontal Mapping (HM) (Reynolds, 1997). The interpretation of VES curves assumes one-dimensional (1-D) horizontally layered resistivity models (Zohdy, 1989). This traditional method has been used in hydrogeological and engineering applications to delineate useful geological situations such as mapping of water table, depth to bedrock, layer thicknesses and so on because the subsurface resistivity changes only with depth (vertical direction) but with no change in the horizontal direction.

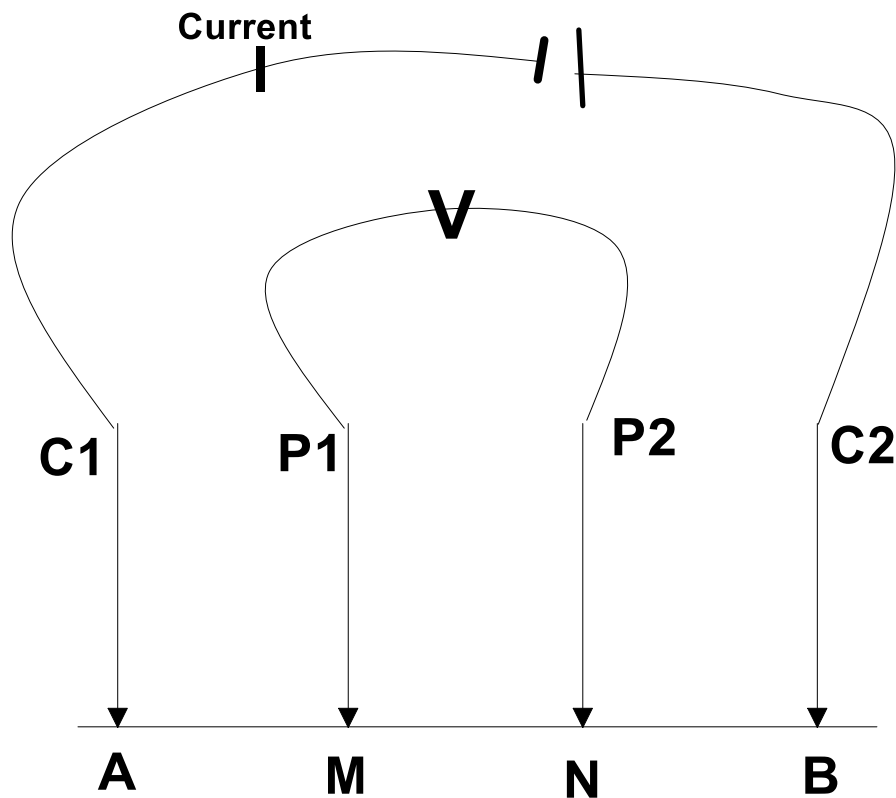


Fig. 2.5 A Conventional collinear four electrode arrangement to measure the subsurface resistivity.

Horizontal profiling or CST is another classical technique, where the four electrodes are moved along the survey line while the spacing between the electrodes remains fixed. And in this case, information about lateral changes in the subsurface resistivity is detected and measured but it cannot detect vertical resistivity changes (Loke, 2011). The measurements obtained are interpreted qualitatively to map the location of vertical structures, such as faults and the overburden thickness. Horizontal mapping (combining several CST profiles) is useful to map lateral resistivity variations (Reynolds, 1997). The limitation of this resistivity sounding method is that only horizontal (lateral) subsurface resistivity changes are measured but no change in the depth.

### **2.3.2b Two and three-dimensional resistivity methods**

Since the 1-D resistivity sounding method is limited to vertical (depth) changes in resistivity and it does not account for horizontal (lateral) changes in the subsurface resistivity. Then, a 2-Dimensional (2-D) model of subsurface resistivity changes in both vertical and horizontal direction is needed to accurately interpret the subsurface geology. In this case, the resistivity does not change in the direction perpendicular to the survey. The more accurate model is 3-Dimensional (3-D) where the resistivity changes in the three orthogonal direction that is in vertical, horizontal and direction perpendicular to the survey line.

The cost of survey is a major factor considered when choosing survey types and keeping the accuracy down in some quarters. Typical 1-D resistivity surveys involve about 10 to 25 readings, while 2-D resistivity surveys about 100 to 1000 measurements. In comparison, 3-D resistivity surveys usually involve several thousand of measurements. The cost of a typical 2-D survey could be several times the cost of a 1-D sounding survey and is probably comparable with a seismic survey. In many geological situations, 2-D electrical imaging surveys can give useful results that are complementary to the information obtained by other geophysical method (Loke, 2011).

#### **2.3.2b(i) Multi-electrode resistivity systems: electrical resistivity tomography**

One of the new developments in recent years is the use of 2-D electrical resistivity tomography surveys to map areas with moderately complex geology (Griffiths & Barker, 1993). This type of survey is usually carried out using a large number of electrodes connected to a multi-core cable. The arrival of this automated multi-electrode resistivity systems has led to rapid and efficient of resistivity data acquisition. It involves the use of multi-electrodes attached to a resistivity system

connected to a laptop microcomputer with an electronic switching unit that automatically select the relevant type of electrode array to use for 2-D and 3-D measurements.

The change of resistivity in both space and time is measured in 4-D surveys (Loke et al., 2013). This is done by using time-lapse 3-D resistivity technique to obtain a 4-D resistivity data (Chambers et al., 2014). It involves taking repeated measurements at different times in the same 2-D survey line or 3-D survey grid. These improvements provide more detailed information than the 1-D resistivity sounding, horizontal profiling and mapping. It has been adopted in areas prone to landslides (Supper et al., 2008), movement of water in aquifers (Cassiani et al., 2009) and monitoring of dam sites (Sjödahl et al., 2008). Recently, automated systems have been introduced for monitoring transient phenomena that require automated data acquisition. These types of sophisticated systems have emerged lately as a new technology for embankment warning systems (Gunn et al., 2010, 2015). Automated time-Lapse Electrical Resistivity Tomography (ALERT-ME) is a fully automated data acquisition developed to be remotely deployed for taking measurements. The system is powered by renewable energy and controlled through wireless telemetry (GPRS) to communicate with an office-based Personal Computer (PC), providing a 24h monitoring system as shown in **Figure 2.6 below**. A number of researchers have used ERT to map water content changes in earthworks embankments because modern multi-electrode systems can be effectively used to map changes in water content of such embankments (Gunn et al., 2015, 2018). For example, when seasonal changes in water content controls the seasonal resistivity changes, water content anomalies can be extracted from time-lapse measurements (**Fig. 2.7**) and it can be used as early warning of moisture build up in engineered earthworks (Chambers et al., 2009).